Article

Rational Design of Macrometallocyclic Trinuclear Complexes with Superior π-Acidity and σ-Basicity

Sammer M. Tekarli, Thomas R. Cundari, and Mohammad A. Omary

J. Am. Chem. Soc., **2008**, 130 (5), 1669-1675 • DOI: 10.1021/ja076527u

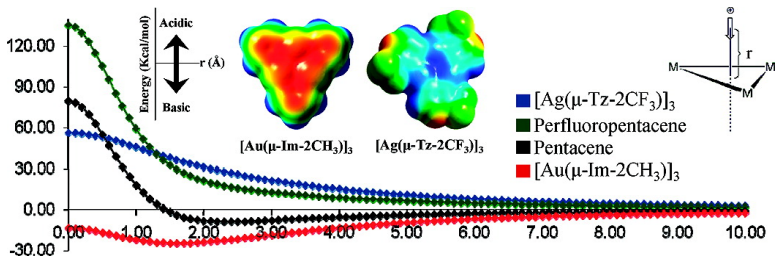

More About This Article

Additional resources and features associated with this article are available within the HTML version:

- Supporting Information
- Links to the 3 articles that cite this article, as of the time of this article download
- Access to high resolution figures
- Links to articles and content related to this article
- Copyright permission to reproduce figures and/or text from this article

View the Full Text HTML

J|A|C|S
ARTICLES
Published on Web 01/15/2008

Rational Design of Macrometallocyclic Trinuclear Complexes with Superior π-Acidity and π-Basicity

Sammer M. Tekarli, Thomas R. Cundari,* and Mohammad A. Omary*

Department of Chemistry, Center for Advanced Scientific Computing and Modeling (CASCaM), University of North Texas, Denton, Texas 76203

Received August 29, 2007; E-mail: tomc@unt.edu; omary@unt.edu

Abstract: Density functional theory (DFT) has been used to assess the π-acidity and π-basicity of metal−organic trimetallic macromolecular complexes of the type $[M(\mu\text{-}L)]_3$, where M = Cu, Ag, or Au and L = carbeniate, imidazolate, pyridiniate, pyrazolate, or triazolate. The organic compounds benzene, triazole, imidazole, pyrazole, and pyridine were also modeled, and their substituent effects were compared to those of the coinage metal trimers. Our results, based on molecular electrostatic potential surfaces and positive charge attraction energy curves, indicate that the metal−organic macromolecules show superior π-acidity and -basicity compared to their organic counterparts. Moreover, the metal−organic cyclic trimers are found to exhibit π-acidity and -basicity that can be systematically tuned both coarsely and finely by judicious variation of the bridging ligand (relative π-basicity imidazolate > pyridiniate > carbeniate > pyrazolate > triazolate), metal (relative π-basicity Au > Cu > Ag), and ligand substituents. These computational findings are thus guiding experimental efforts to rationally design novel $[M(\mu\text{-}L)]_3$ materials for applications in molecular electronic devices that include metal−organic field-effect transistors and light-emitting diodes.

Introduction

A cation−π-interaction is a strong, multicenter, presumably primarily noncovalent bonding force between a cation and the π-molecular orbitals of an aromatic structure (Chart 1). This type of interaction has been observed and studied extensively over the past 20 years with organic π-systems.[1−7] Cation−π-interactions play an important role in many areas of chemistry, such as materials design, acid−base chemistry, molecular biology, gas-phase chemistry, and metalloaromaticity.[1−7] For example, Ngola et al. studied the effect of fluorination of cyclophane upon altering the molecular recognition properties of aromatic systems.[7] It was found that fluorination of the benzene rings in cyclophane leads to a decrease in cation binding affinity, which suggested that fluorination alters the electrostatic binding properties of the cyclophane aromatic rings.[7] Gallivan and Dougherty reported that cation−π-interactions occur between the cationic side chains of lysine, arginine, and tyrosine and the aromatic side chains of phenylalanine, tyrosine, and tryptophan in proteins. These researchers concluded that tryptophan has the strongest cation−π-interaction as compared to the other aromatic amino acids.[4] Other experimental studies of cation−π-interactions have been made in both the gas phase and in aqueous media.[8]

Chart 1. A Model of Basic Cation−π-Interaction Showing a Generic Cation Placed over Benzene along the 6-Fold Axis

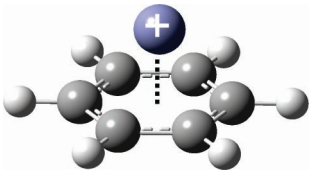

Dougherty and co-workers have reported a computational study of metal cation−π-interactions.[6] Computational chemistry studies of the binding energies of sodium cation (Na^+) to the π-face of several aromatic compounds, such as benzene, fluorobenzene, *p*-difluorobenzene, aniline, pyridine, indicate that inductive effects play a more important role than resonance effects in the binding of Na^+ to the π face of the aromatic ring.[5] This result is particularly interesting, as one expects inductive effects such as electronegativity to be primarily transmitted through the σ-framework of the aromatic moiety. The study by Dougherty et al. for aromatic molecules inspired us to conduct an investigation of cation−π-interactions for the macrometallocyclic trinuclear complexes of the coinage metals.

Cyclic trinuclear complexes of d^{10} monovalent coinage metal ions — cyclo-$M_3(\mu\text{-}L)_3$ — possess planar, nine-membered $M_3N_xC_{6-x}$ rings. These complexes represent a significant class of coordination compounds with a remarkable range of properties that are relevant for a plethora of fundamental and applied areas of chemistry that include π vs Brønsted vs Lewis acid−base chemistry, metalloaromaticity, metallophilic and excimeric bonding, supramolecular host/guest chemistry, and metal−organic optoelectronics. For example, several groups including

(1) Dougherty, D. A. *Science* **1996**, *271*, 163.
(2) Gallivan, J. P.; Dougherty, D. A. *J. Am. Chem. Soc.* **2000**, *122*, 870.
(3) Zacharias, N.; Dougherty, D. A. *Trends Pharmacol. Sci.* **2002**, *23*, 281.
(4) Gallivan, J. P.; Dougherty, D. A. *Proc. Natl. Acad. Sci. U.S.A.* **1999**, *96*, 9459.
(5) Mecozzi, S.; West, A. P., Jr.; Dougherty, D. A. *J. Am. Chem. Soc.* **1996**, *118*, 2307.
(6) Mecozzi, S.; West, A. P., Jr.; Dougherty, D. A. *Proc. Natl. Acad. Sci. U.S.A.* **1996**, *93*, 10566.
(7) Ngola, S. M.; Dougherty, D. A. *J. Org. Chem.* **1998**, *63*, 4566.
(8) Ma, J. C.; Dougherty, D. A. *Chem. Rev.* **1997**, *97*, 1303.

10.1021/ja076527u CCC: $40.75

Chart 2. Structures of Representative $[M(\mu\text{-}L)]_3$ Cyclotrimers

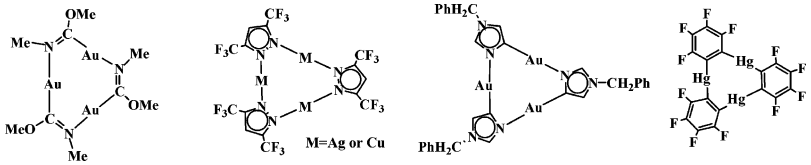

our own have reported remarkably rich photoluminescence, supramolecular, acid−base, and donor−acceptor properties for a variety of cyclotrimeric d^{10} complexes such as those illustrated in Chart 2.[9,10] Boldyrev and Wang[11a] have recently reviewed metalloaromaticity, focusing on main group species but also providing some discourse on coinage metals. Other interesting studies in the field of metalloaromaticity include the combined theoretical−experimental investigation of $Cu_3C_4^-$ by Alexandrova et al.[11b] and the work by Tsipis et al., which suggests that cyclo-$M_n(\mu\text{-}H)_n$ models (M = Au, Ag, Cu; $n = 3-6$) are aromatic![11c]

A systematic study of π-acidity and -basicity is important in determining the electronic and molecular structures of π-coordination of $M_3N_xC_{6-x}$ macrocyclic rings with one another, with cations and anions, with organic aromatic substrates such as benzene and larger polycyclic rings (e.g., naphthalene, pyrene, and pentacene), with apo- and metal-containing porphyrins and phthalocyanines, and with several other possible classes of planar organic and metal−organic molecules known for their electron-rich or electron-poor properties. Some of these reactivities have been already realized. For example, the Balch group showed that Au(I)−carbeniate complexes (such as the first structure in Chart 2) form deeply colored charge-transfer adducts with the organic acceptors polynitro-9-fluorenones.[10c] Fackler et al. reported supramolecular assemblies involving electron-rich cyclic trinuclear gold(I) complexes with various electron-poor entities that included heavy-metal cations (Tl^+ and Ag^+), a trinuclear Hg(II) complex (Chart 2), and organic Lewis acids (C_6F_6 and $C_{10}F_8$) and electron acceptors (TCNQ).[10a,b,g] These

Chart 3. Bridging Ligands (L) in Cyclo-$M_3(\mu\text{-}L)_3$ That Are Studied in This Paper

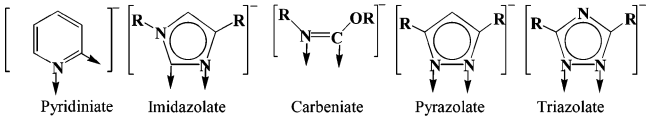

authors also reported structural evidence (based on 2-D NMR) of acid−base π-stacking in solution for binary trinuclear complexes of Hg(II) and Au(I).[12] Gabbaï and co-workers showed that a trinuclear Hg(II) complex (Chart 2) forms 1:1 π-acid−base stacks with a variety of arenes and sensitizes their phosphorescence at room temperature.[10j−n]

Significant optoelectronic applications are anticipated for this class of trimers in view of the fascinating luminescence properties reported and their sensitivities to multiple factors such as temperature, solvent, molecular structure, and concentration. In collaboration with the Dias group, we have reported studies of the effect of changing the metal (Cu, Ag, and Au) on the supramolecular structure and acid−base stacking of trinuclear pyrazolates. It was found based on DFT calculations that the relative basicity of these trinuclear compounds was Ag ≪ Cu < Au.[9a] In support of this computational prediction, which was made on the basis of molecular electrostatic potentials (MEP, vide infra), the synthesis of a π-stack of toluene and $\{[3,5\text{-}(CF_3)_2Pz]Au\}_3$ was attempted and successfully realized.[9a] Subsequent studies by the Dias group have led to isolation of several π-acid−base adducts of $\{[3,5\text{-}(CF_3)_2Pz]Ag\}_3$ with unsubstituted and substituted benzene.[10d,e]

This paper reports a comprehensive computational study of the π-acid−base properties of cyclic trinuclear complexes of monovalent coinage metals with all the bridging ligands that have been experimentally investigated thus far (shown in Chart 3). The calculations assess the interplay of the effect of the ligand, coinage metal, and substituents in cyclo-$M_3(\mu\text{-}L)_3$ vis-à-vis the rational design of π-acids and bases with tunable properties for various optoelectronic applications. A comparison is also presented with organic analogues, both in terms of fundamental aspects vs the cation−π-systems studied by Dougherty et al.[1−8] and applied aspects vs molecules commonly used in organic electronics.

Computational Methods

Geometry optimizations of the bridging ligands and of the trimer complexes $[M(\mu\text{-}L)]_3$ [where M = Cu, Ag, or Au; L = carbeniate (Cb), imidazolate (Im), pyrazolate (Pz), pyridiniate (Py), and triazolate (Tz)] were performed using the Gaussian 03 suite of programs.[13] All calculation were done using the B3LYP[14−16] hybrid functional in

(9) (a) Omary, M. A.; Rawashdeh-Omary, M. A.; Gonser, M. W.; Elbjeirami, O.; Grimes, T.; Cundari, T. R.; Diyabalanage, H. V. K.; Gamage, C. S. P.; Dias, H. V. R. *Inorg. Chem.* **2005**, *44*, 8200. (b) Dias, H. V. R.; Diyabalanage, H. V. K.; Eldabaja, M. G.; Elbjeirami, O.; Rawashdeh-Omary, M. A.; Omary, M. A. *J. Am. Chem. Soc.* **2005**, *127*, 7489. (c) Vorontsov, I. I.; Kovalevsky, A. Yu.; Chen, Y-S.; Graber, T.; Novozhilova, I. V.; Omary, M. A.; Coppens, P. *Phys. Rev. Lett.* **2005**, *94*, 193003. (d) Grimes, T.; Omary, M. A.; Dias, H. V. R.; Cundari, T. R. *J. Phys. Chem. A* **2006**, *110*, 5823. (e) Yang, C.; Messerschmidt, M.; Coppens, C.; Omary, M. A. *Inorg. Chem.* **2006**, *45*, 6592. (f) Yang, C.; Wang, X.; Omary, M. A. *J. Am. Chem. Soc.* **2007**, *129*, 15454.

(10) (a) Burini, A.; Mohamed, A. A.; Fackler, J. P., Jr. *Comm. Inorg. Chem.* **2003**, *24*, 253. (b) Omary, M. A.; Mohamed, A. A.; Rawashdeh-Omary, M. A.; Fackler, J. P., Jr. *Coord. Chem. Rev.* **2005**, *249*, 1372. (c) Olmstead, M. M.; Jiang, F.; Attar, S.; Balch, A. L. *J. Am. Chem. Soc.* **2001**, *123*, 3260. (d) Dias, H. V. R.; Gamage, C. S. P.; Keltner, J.; Diyabalanage, H. V. K.; Omari, I.; Eyobo, Y.; Dias, N. R.; Roehr, N.; McKinney, L.; Poth, T. *Inorg. Chem.* **2007**, *46*, 2979. (e) Dias, H. V. R.; Gamage, C. S. P. *Angew. Chem., Int. Ed.* **2007**, *46*, 2192. (f) White-Morris, R. L.; Olmstead, M. M.; Attar, S.; Balch, A. L. *Inorg. Chem.* **2005**, *44*, 5021. (g) Rawashdeh-Omary, M. A.; Omary, M. A.; Fackler, J. P., Jr.; Galassi, R.; Pietroni, B. R.; Burini, A. *J. Am. Chem. Soc.* **2001**, *123*, 9689. (h) Mezei, G.; Raptis, R. G.; Telser, J. *Inorg. Chem.* **2006**, *45*, 8841. (i) Vaughan, L. G. *J. Am. Chem. Soc.* **1970**, *11*, 730. (j) Haneline, M. R.; Gabbaï. F. P. *Angew. Chem., Int. Ed.* **2004**, *43*, 5471−5474. (k) Omary, M. A.; Kassab, R. M.; Haneline, M. R.; Elbjeirami, O.; Gabbaï, F. P. *Inorg. Chem.* **2003**, *42*, 2176. (l) Burress, C.; Elbjeirami, O.; Omary, M. A.; Gabbaï, F. P. *J. Am. Chem. Soc.* **2005**, *127*, 12166. (m) Elbjeirami, O.; Burress, C. N.; Gabbaï, F. P.; Omary, M. A. *J. Phys. Chem. C* **2007**, *111*, 9522−9529. (n) Burress, C. N.; Bodine, M. I.; Elbjeirami, O.; Reibenspies, J. H.; Omary, M. A.; Gabbaï, F. P. *Inorg. Chem.* **2007**, *46*, 1388.

(11) (a) Boldyrev, A. I.; Wang, L. *Chem. Rev.* **2005**, *105*, 3716. (b) Alexandrova, A. N.; Boldyrev, A. I.; Zhai, H.; Wang, L. *J. Phys. Chem. A* **2005**, *109*, 562. (c) Tsipis, C. A.; Karagiannis, E. E.; Kladou, P. F.; Tsipis, A. C. *J. Am. Chem. Soc.* **2004**, *126*, 12916.

(12) Burini, A.; Fackler, J. P., Jr.; Galassi, R.; Macchioni, A.; Omary, M. A.; Rawashdeh-Omary, M. A.; Pietroni, B. R.; Sabatini, S.; Zuccaccia, C. *J. Am. Chem. Soc.* **2002**, *124*, 4570.

(13) Frisch, M. J.; et al. *Gaussian 03*, Revision C.02; Gaussian, Inc.: Wallingford, CT, 2004.

(14) Lee, C.; Yang, W.; Parr, R. G. *Phys. Rev. B* **1988**, *37*, 785.

(15) Becke, A. D. *Phys. Rev. A* **1988**, *38*, 3098.

Chart 4. Approach Used in PCA Computations for Cyclo-$M_3(\mu\text{-}L)_3$[a]

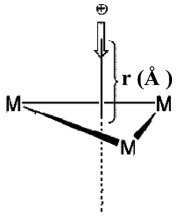

[a] For clarity purposes, only the metals that form the nine-membered metallacyclic ring are shown here, but the computations involved the full ligands. See Charts 2 and 3.

conjunction with the CEP-31G(d) basis set,[17−19] where the (d) signifies addition of a d-polarization function to main group elements. The CEP-31G pseudopotentials include scalar relativistic effects as they are derived from Dirac−Hartree−Fock all-electron wave functions; in our modeling of coinage metal chemistry, we have seen no diminution in accuracy as one traverses from copper to gold. Molecular electrostatic potential (MEP) surfaces were plotted using the GaussView03 program;[20] values for the isosurfaces are denoted in the figure captions. The HOMO and LUMO energies were determined by the time-dependent DFT (TD−DFT) method.

The proton affinities of the neutral bridging ligands (LH) were calculated from B3LYP/CEP-31G(d)-determined enthalpies (1 atm, 298.15 K, unscaled vibrational frequencies) in order to determine their intrinsic Lewis (i.e., σ) acid−base properties, viz.

$$\text{proton affinity } (L^-) = H_{LH} - (H_{L-} + H_{H+})$$

Using the GAMESS program,[21,22] positive charge attraction (PCA) calculations were made by placing a positive charge along the 3-fold axis normal to the M_3 plane and passing through the center of the compound. The positive charge was moved through different distances (r) ranging from 10 Å above to 10 Å below (in 0.1 Å increments) the plane of the ring, as depicted in Chart 4.

Results and Discussion

1. Molecular Electrostatic Potentials of Cyclo-$M_3(\mu\text{-}L)_3$ Trimers. Three chemical effects are studied to assess the π-acidity/basicity of the cyclic trinuclear cyclo-$M_3(\mu\text{-}L)_3$ compounds on the basis of MEP: bridging ligand (L), metal (M), and substituents (R in Chart 3) on the ligand. For the sake of comparison with the present metal−organic π-acids/bases, prototypical organic aromatic molecules are also evaluated using the same computational approaches.

a. Bridging Ligands (L) and MEP. An assessment of the impact of the bridging ligand (L) on the π-acid−base properties of cyclo-$M_3(\mu\text{-}L)_3$ is made. Unsubstituted ligands are used for this purpose (R = H in Chart 3). We first describe our attempts to establish a relationship between the proton affinity (PA)—and thus the intrinsic Brønsted basicity—of each anionic bridging ligand (L^-) and the resulting acid/base properties of cyclo-$M_3(\mu\text{-}L)_3$ in a π−cation situation. We find from B3LYP/CEP-31G(d) calculations that the relative Lewis basicity is as follows: triazolate (PA = 340.3 kcal/mol) > pyrazolate (PA = 359.2 kcal/mol) > carbeniate (PA = 391.2 kcal/mol) > imidazolate (PA = 396.2 kcal/mol) > pyridiniate (PA = 406.6 kcal/mol). These values are in good accord with the available experimental gas-phase PAs: triazolate (PA = 344.2 ± 2.1), pyrazolate (PA = 353.7 ± 2.1), imidazolate (H^+ removed from ligating N atom, PA = 350.1 ± 2.1), and pyridiniate (PA = 391.0 ± 2.5).[23−25] The calculated proton affinities indicate that the energy of removing a proton from a carbon (i.e., for pyridiniate, imidazolate, and carbeniate) is considerably higher (>30 kcal/mol) than removing a proton from a nitrogen (i.e., for pyrazolate and triazolate), which is inherently reasonable on the basis of electronegativity arguments.

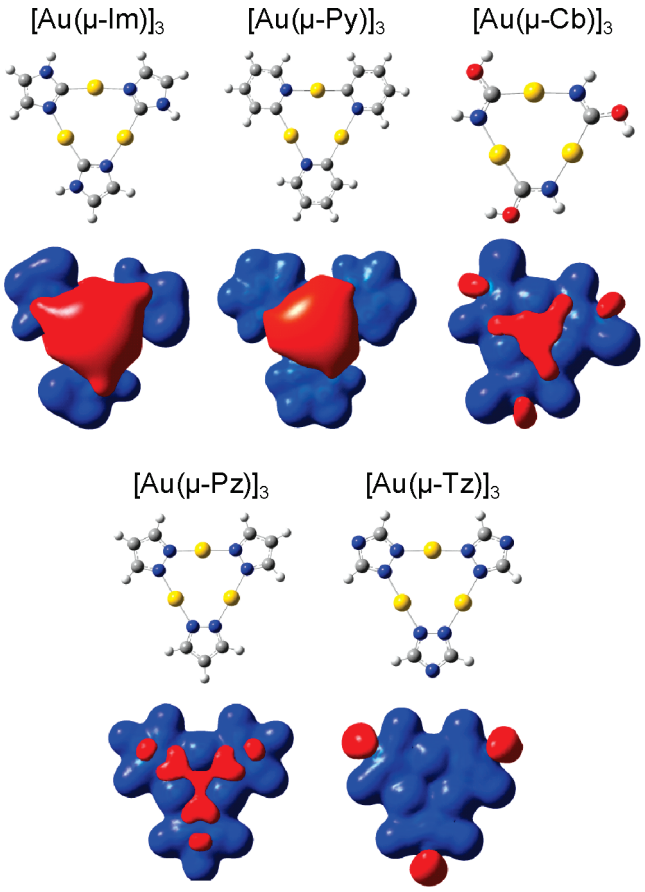

Figure 1. MEP surfaces showing the relative π-basicity of cyclo-$M_3(\mu\text{-}L)_3$ cyclotrimers as a function of the bridging ligand; isosurface value = 0.02.

It is now imperative to assess whether differences in the acidity of LH (and thus the basicity of its conjugate base, L^-) are manifested in coinage metal cyclo-$M_3(\mu\text{-}L)_3$ complexes. Such a link, if established, is potentially very valuable, as it would provide a design criterion for rationally tuning the π-acid/base properties of metal−organic cyclotrimers. The calculated MEP surfaces of cyclo-$M_3(\mu\text{-}L)_3$ are shown in Figure 1 and indicate the relative π-basicity of the trinuclear compounds as a function of the bridging ligands. To minimize chemical

(16) Stephens, P. J.; Devlin, F. J.; Chabalowski, C. F.; Frisch, M. J. *J. Phys. Chem.* **1994**, *98*, 11623.
(17) Cundari, T. R.; Stevens, W. J. *J. Chem. Phys.* **1993**, *98*, 5555.
(18) Stevens, W. J.; Krauss, M.; Basch, H.; Jasien, P. G. *Can. J. Chem.* **1992**, *70*, 62.
(19) Stevens, W.; Basch, H.; Krauss, J. *J. Chem. Phys.* **1984**, *81*, 6026.
(20) Dennington, R., II; Keith, T.; Millam, J.; Eppinnett, K.; Hovell, W. L.; Gilliland, R. *GaussView*; Semichem Inc.: Shawnee Mission, KS, 2003.
(21) Gordon, M. S.; Schmidt, M. W. *Theory and Applications of Computational Chemistry: The First Forty Years*; Elsevier: Amsterdam, 2005.
(22) Schmidt, M. W.; Baldridge, K. K.; Boatz, J. A.; Elbert, S. T.; Gordon, M. S.; Jensen, J. H.; Koseki, S.; Matsunaga, N.; Nguyen, K. A.; Su, S.; Windus, T. L.; Dupuis, M.; Montgomery, J. A. *J. Comput. Chem.* **1993**, *14*, 1347.
(23) Linstrom, P. J., Mallard, W.G., Eds., *NIST Chemistry WebBook, NIST Standard Reference Database Number 69*, National Institute of Standards and Technology: Gaithersburg, MD, 2005 (http://webbook.nist.gov).
(24) Meot-ner, M.; Kafafi, S. A. *J. Am. Chem. Soc.* **1988**, *110*, 6297.
(25) Taft, R.; Anvia, F.; Taagepera, M.; Catalan, J.; Elgueroy, J. *J. Am. Chem. Soc.* **1986**, *108*, 3237.

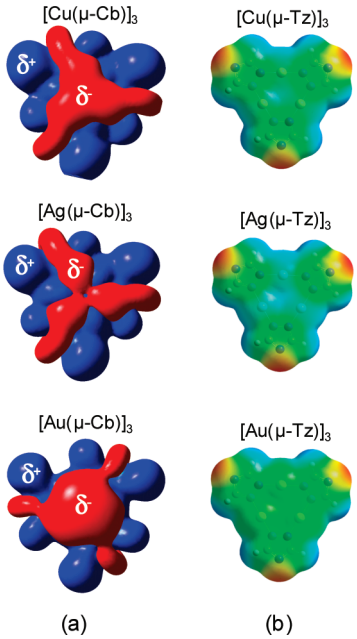

Figure 2. MEP surfaces showing the relative π-basicity of cyclo-$M_3(\mu\text{-}L)_3$ cyclotrimers as a function of the metal with L = (a) carbeniate and (b) triazolate. MEP surfaces are shown both in space (with positive and negative regions shown in blue and red, respectively) and mapped on electron densities of the molecule (MEP color scale is such that basicity increases in the direction blue → green → yellow → orange → red).

variables, the metal was chosen to be gold for the set of initial calculations. Note that the red region represents the most basic region of the trimer, whereas the blue region represents the least basic region of the molecule. *From the distribution of the MEP surfaces, it is clear that these cyclo-$M_3(\mu\text{-}L)_3$ are multicentered, π-acids/bases, presumably with synergistic interactions among the coinage metals (mediated by L), as opposed to simple assemblages of three Lewis (σ) acids/bases.*

Figure 1 shows that the calculated relative π-basicity is [Au(μ-Im)]$_3$ > [Au(μ-Py)]$_3$ > [Au(μ-Cb)]$_3$ > [Au(μ-Pz)]$_3$ > [Au(μ-Tz)]$_3$. Indeed, it is apparent from Figure 1 that acid−base properties can substantially change with ligand modification, giving [Au(μ-Im)]$_3$ the MEP profile of a base while [Au(μ-Tz)]$_3$ is clearly acidic in its comportment. The same trend in π-acidity/basicity of cyclo-$M_3(\mu\text{-}L)_3$ is followed when using Cu and Ag as the coinage metal (not shown). Both the results of the calculated proton affinities and the molecular electrostatic potential surfaces are comparable at least for the weakest and strongest base, and thus, the former give valuable insight as to how the intrinsic acid−base properties of the ligand are transmitted through the cyclo-$M_3(\mu\text{-}L)_3$ framework to produce a multicentered π-acid/base. For example, the PA for imidazolate = 340.3 kcal/mol, whereas the PA for triazolate is much higher, 396.2 kcal/mol; this result for the isolated anionic ligand is consistent with [Au(μ-Im)]$_3$ being a π-base while [Au(μ-Tz)]$_3$ is a π-acid. The results from calculated proton affinities of L^- are, therefore, a simple assessment tool for the π-acidity/basicity of the trimer and support the contention that the ligand L has a more than nominal role in the overall chemistry of these coinage metal cyclotrimers.

b. Metals (M) and MEP. Figure 2 shows the effect of varying the metal on the π-acidity and -basicity of unsubstituted carbeniate and triazolate cyclotrimers.

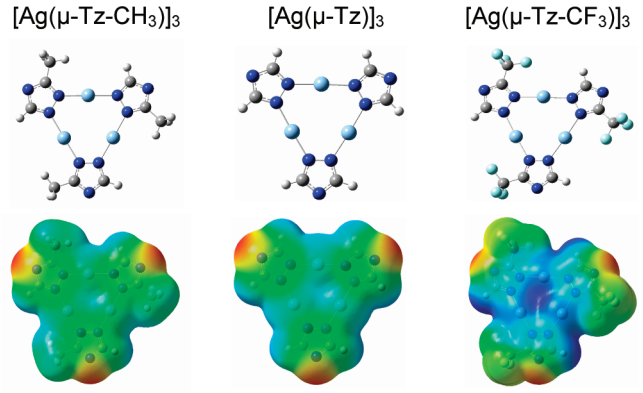

Figure 3. Relative π-basicity of silver triazolate trimers as a function of the ligand substituents; isosurface value = 0.0004.

The metal effect on π-basicity is Au (most basic) > Cu > Ag (least basic). This trend is the same as that reported earlier[9] for the pyrazolate trimers. The MEP surfaces in Figure 2 have smaller isosurface values than those used in Figure 1; the choice of a smaller isosurface value is a reflection of the great impact of the ligands in modifying the π-acid/base properties of cyclo-$M_3(\mu\text{-}L)_3$ complexes. While other bridging ligands may be more or less "tunable" in their π-acid/base properties by modification of the coinage metal, the order of π-basicity of cyclo-$M_3(\mu\text{-}L)_3$ is always Au > Cu > Ag for all L ligands investigated (Chart 3).

c. Substituents and MEP. It is apparent from the experimental literature that the electronic factor likely plays a greater role than the steric factor of the substituents on the bridging ligand L in determining the structural, chemical, and photophysical properties of cyclo-$M_3(\mu\text{-}L)_3$ complexes. For example, Dias et al. have found that replacing alkyl substituents such as Me and ^{i}Pr with one or two CF_3 substituents in the 3- and 5-positions alters the stacking of Cu(I) pyrazolate trimers from dimer-of-trimer structures with short intertrimer distances to chain-of-trimer structures with long intertrimer distances.[9b]

In this section, we seek to investigate the electronic consequences of substituent modification on the π-acid−base properties through the use of the MEP. The inductive effect (as seen above) is an obvious factor with respect to the role of the substituent in modifying the acid/base properties of cyclo-$M_3(\mu\text{-}L)_3$. An electron-withdrawing group on the bridging ligands is expected to cause the trimer to become more π-acidic. The more electron-withdrawing the group, the more acidic the trimer is expected to become. However, the substituent is typically separated from the metal by several bonds and thus it is reasonable to ask, to what extent are the inductive effects of the substituents manifest in the π-acid/base properties of the resultant trimeric complex? Figure 3 shows a comparison of the MEP among an electron-withdrawing (i.e., trifluoromethyl), an electron-donating (i.e., methyl), and an electron-neutral (i.e., H) bridging ligand substituent. It is seen that π-acidity increases noticeably with the increasing strength of the electron-withdrawing group. *Thus, Figure 3 makes it apparent that inductive effects can be transmitted through the molecular skeleton to be manifested in the π-acidity/basicity, and thus, ligand substituents are very useful to fine-tune the π-acidity/basicity of the trimer.*

2. Positive Charge Attraction (PCA) along the Three-Fold Axis of Cyclo-$M_3(\mu\text{-}L)_3$. From the MEP results in the previous section, it is evident that the π-acidity/basicity is "centered"

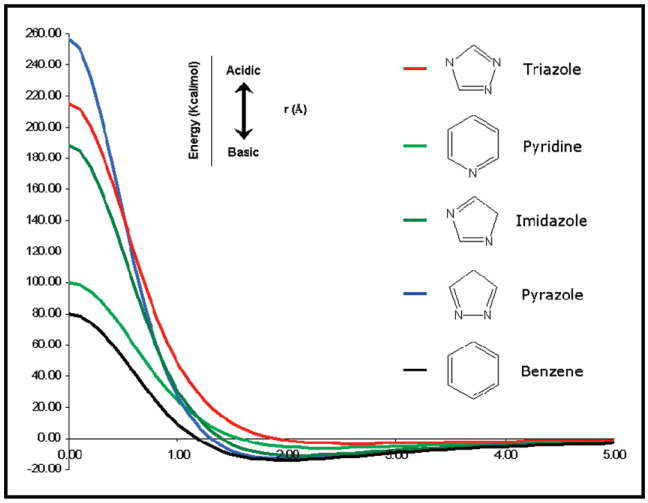

Figure 4. Positive charge attraction (PCA) energy curve showing the relative π-basicity of the organic compounds benzene, pyridine, imidazole, triazole, and pyrazole.

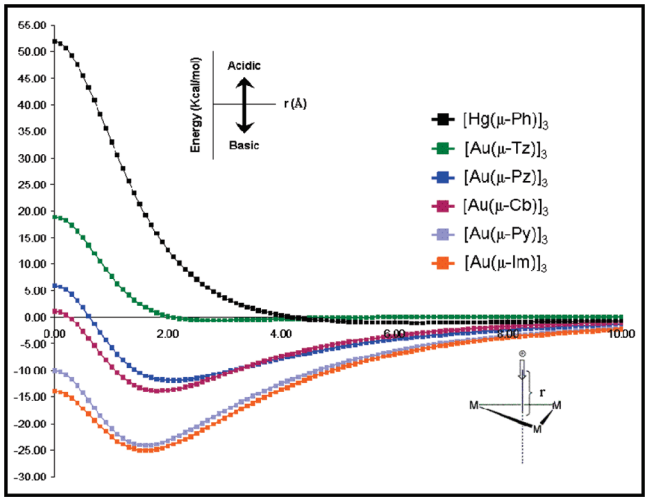

Figure 5. Positive charge attraction energy curve showing the relative π-basicity of $M_3(\mu\text{-L})_3$ metal−organic trimers as a function of the bridging ligand (L). See Chart 3 for ligand designations.

not at a coinage metal atom but rather at the centroid of the $M_3N_xC_{6-x}$ ring (Figures 1−3). Therefore, calculations were made to quantify the attraction of a positive point charge placed along the 3-fold axis (Chart 4) at various distances from the centroid of the $M_3N_xC_{6-x}$ ring. As before, the same three chemical effects—bridging ligand, metal, and the bridging ligand substituents—are studied using positive charge attraction energy. The positive charge attraction calculations should provide a quantitative way to assess the extent of cation−π-interactions and π-acid/base properties of cyclo-$M_3(\mu\text{-L})_3$, as studied in the following section in comparison to selected organic prototypes.

a. Metal, Bridging Ligands, Substituents, and PCA. As shown in Chart 4, the *x*-axis represents the distance in Å from the $M_3N_xC_{6-x}$ ring centroid. Hence, in a PCA plot, the *y*-axis represents the attraction energy in kcal/mol, thus defining a π-base ($y < 0$) or a π-acid ($y > 0$), Figure 4. Similarly, the same PCA approach is assessed for the attraction of a positive charge with the centroids of the rings in organic aromatic molecules, and the results are correlated with those previously reported by Dougherty et al.[1,6] For the organic molecules, the π-basicity order indicated by the PCA plot in Figure 4 is benzene > pyrazole > imidazole > pyridine > triazole.

Moving to the coinage metal cyclotrimers, the MEP and PCA (cf. Figures 1 and 5) analyses of the bridging ligands show a consistent trend: as the positive charge attraction energy increases, the π-basicity increases. Further analyses of PCA curves like those in Figure 5 show that the minima in attractive PCA curves for π-bases correspond to a distance between the positive charge and the center of the cyclotrimers of ca. 1.5−2.0 Å. Interestingly, unlike the organic counterparts, the PCA is attractive at the centroids of some metal−organic trimers, such as $[Au(\mu\text{-Im})]_3$ and $[Au(\mu\text{-Py})]_3$ (−14.0 and −10.0 kcal/mol, respectively), which implies that a relatively small cation (e.g., Li^+ or Na^+) may bind in the $M_3N_xC_{6-x}$ ring plane of the trimer.

As for the other two modifiable chemical components of these coinage metal trimers—the metal and the ligand substituents—analysis of the quantitative results from the PCA curves leads to conclusions that mimic the qualitative results derived from the MEP calculations. *Therefore, there is a direct correlation between the MEP and PCA results.* This is not surprising, due

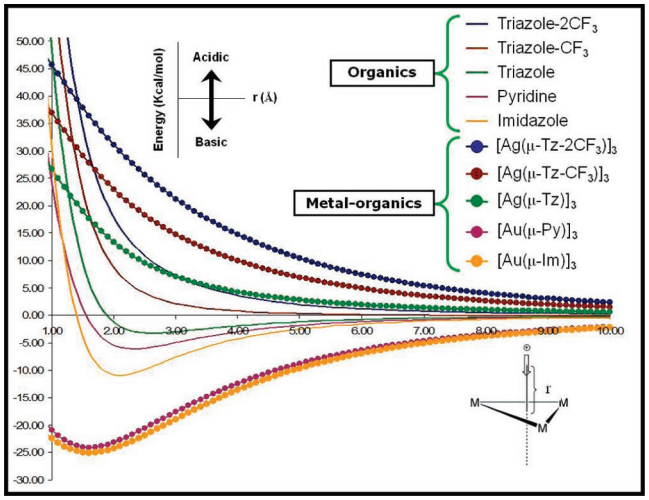

Figure 6. Positive charge attraction energy illustrates examples of relative π-basicity of the organic compounds vs the metal−organic trimer complexes.

to the electrostatic nature of the cation−π-interaction, which makes its evaluation via the PCA approach a function of the extent of π-basicity inferred from the MEP analysis.

b. Organic versus Metal−Organic PCA Curves. Positive charge attraction curves were generated for an assortment of arene compounds, including ones studied earlier in Dougherty's work (e.g., benzene, cyanobenzene, aniline),[6] neutral aromatic molecules whose anions form neutral cyclotrimers with monovalent coinage metal ions [e.g., imidazole, pyrazole, triazole, 3,5-*bis*(trifluoromethyl)triazole, and 3,5-(dimethyl)triazole], as well as other arenes that are known to have applications in molecular electronic devices (e.g., pentacene and perfluoropentacene). The PCA curves are compared for these arenes with those for coinage metal cyclotrimers (Figure 6). *What is striking from these results is that, at typical π-cation bonding distances (~2−3 Å), the metal−organic trimers easily span both ends of the acidity and basicity scale of the organic congeners (Figure 6).* The complex $[Ag(\mu\text{-Tz-}2CF_3)]_3$ is much more π-acidic compared with the organic analogue 3,5-bis(trifluoromethyl)-triazole. Likewise, $[Au(\mu\text{-Py})]_3$ is substantially more π-basic than pyridine (Figure 6). These results thus further support the

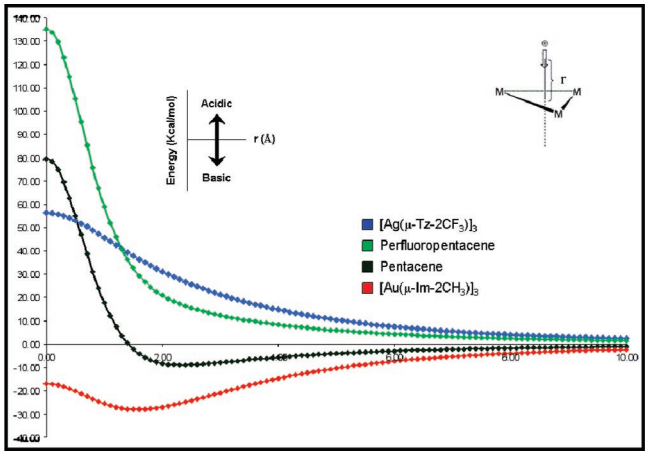

Figure 7. Positive charge attraction energy illustrates examples of relative π-basicity of the pentacene and perfluoropentacene and the best π-base and π-acid trimer complexes.

emerging theme from this research regarding the synergism among the M and L fragments to influence the resulting π-acidity/basicity of these remarkable coinage metal trimers.

3. Potential for Applications in Molecular Electronics. Another pair of arene compounds, pentacene and perfluoropentacene, were evaluated in terms of their π-acidity/basicity using calculated PCA curves and were compared to the coinage metal trimers. Pentacene, a planar aromatic p-type semiconductor, was chosen for these purposes, as it has been widely studied in relation to organic field-effect transistors (OFETs), materials that have applications such as plastic electronics, electronic papers, and flexible displays.[26] Sakamoto and co-workers have synthesized perfluoropentacene as an n-type semiconductor (a highly sought after material type) to complement the p-type, pentacene, in order to produce bipolar transistors.[26] Impressive electronic (e.g., electron and hole mobilities and on/off ratios) and physical (e.g., stability and lattice match) properties were noted by these researchers for pentacene/perfluoropentacene electronics. Because the conduction of these OFET materials occurs through π- and π*-molecular orbitals, their π-acidity and basicity are obviously relevant.

In the light of the work by Sakamoto and co-workers,[26] here we evaluate the π-acidity/basicity of two among the most π-basic, $[Au(\mu\text{-}Im\text{-}2CH_3)]_3$, and most π-acidic, $[Ag(\mu\text{-}Tz\text{-}2CF_3)]_3$, metal−organic cyclotrimers in comparison with the organic arenes pentacene and perfluoropentacene using the PCA procedure. The results are graphed in Figure 7. *Interestingly, $[Au(\mu\text{-}Im\text{-}2CH_3)]_3$ is found to be much more π-basic than pentacene, and $[Ag(\mu\text{-}Tz\text{-}2CF_3)]_3$ is much more π-acidic than perfluoropentacene.* Hence, the metal−organic coinage metal cyclic trimers appear to be very promising candidates for n- and p-type semiconductors as metal−organic field-effect transistors (MOFETs). We caution, however, that (a) the calculations are carried out for monomeric models while the functional form is a solid-state thin film in which the hopping of charge carriers between packed molecules may not necessarily favor the metal−organic cyclotrimers and (b) the band gap is much smaller for the organic semiconductors while most coinage-metal cyclotrimers are generally wide-band gap materials. *Nevertheless, the findings in this work, as illustrated in Figure 7, suggest that it is worthwhile to investigate the use of the most electron-rich and electron-poor cyclotrimers as MOFETs.*

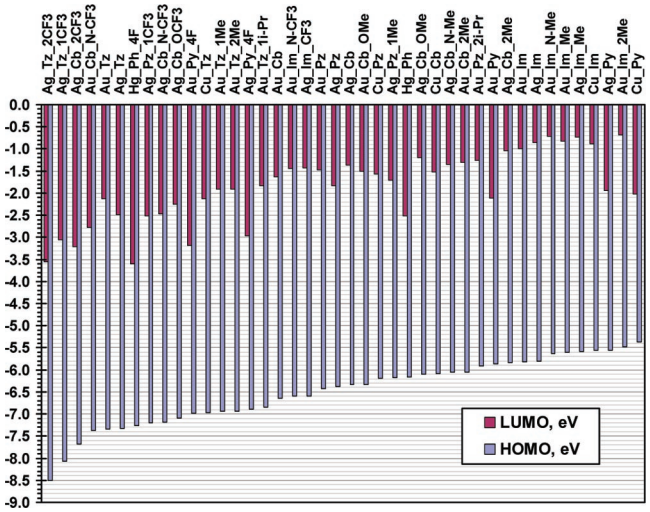

Figure 8. Computational HOMO/LUMO data for various cyclic trimers considered for exciton confinement in OLEDs. The trimer models computed are identified by the "metal_ligand_substituent" combination (e.g., $Ag\_Tz\_2CF_3 = \{\mu\text{-}[3,5\text{-}(CF_3)_2Tz]Ag\}_3$).

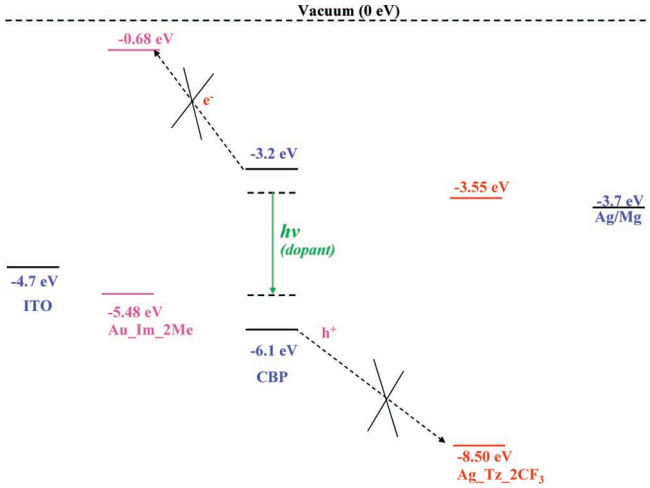

Figure 9. A proposed OLED structure based on conventional host:dopant systems while achieving exciton blocking from both the anode and cathode sides by a π-basic Au trimer (in pink) and a π-acidic Ag trimer (in red), respectively. The common host CBP is 4,4′-*N*,*N*′-dicarbazolebiphenyl.

Another application for the metal−organic cyclotrimers inferred from the computational work herein is exciton blocking in organic light-emitting diodes (OLEDs). This application is illustrated by Figures 8 and 9. Figure 8 shows the HOMO and LUMO energies predicted by TD−DFT calculations for various cyclic trimers. Zhang and Musgrave[27] have recommended on the basis of their survey of HOMO and LUMO energies with a variety of density functionals that, rather than directly calculating the LUMO orbital energy, this quantity is more reliably derived from the HOMO energy plus the HOMO−LUMO gap as obtained from a TD−DFT calculation. This is the approach employed here to obtain LUMO orbital energies. The values are demonstrated to be reliable on the basis of comparison with values determined by experimental methods (UPS, electronic absorption, and cyclic voltammetry) for pentacene and perfluoropentacene,[26] as well as representative

(26) Sakamoto, Y.; Toshiyasu, S.; Koboyashi, M.; Gao, Y.; Fukai, Y.; Inoue, Y.; Sato, F.; Tokito, S. *J. Am. Chem. Soc.* **2004**, *126*, 8138.

(27) Zhang, G.; Musgrave, C. *J. Phys. Chem. A* **2007**, *111*, 1554.

cyclotrimers.[28] For the $[Hg(\mu\text{-}C_6F_4)]_3$ trimer, for example, the computed HOMO and LUMO energies of 7.34 and 3.60 eV, respectively, are in very good agreement with the corresponding experimental values of 7.5 and 3.4 eV.[28] The overall computational data in Figure 8 indicate that the HOMO and LUMO levels of a variety of metal−organic cyclic trimers can be both fine- and coarse-tuned over a large energy range.

The strongly π-acidic cyclo-$M_3(\mu\text{-}L)_3$ are characterized by low-lying LUMO and HOMO orbitals, while the strong π-acids are characterized by high-lying LUMO and HOMO orbitals. The consequence of these findings on OLEDs research is illustrated in Figure 9. The very deep HOMO energies (7.5−8.5 eV) of π-acidic trimers such as the $[Ag(\mu\text{-Tz-}2CF_3)]_3$, $[Ag(\mu\text{-Pz-}2CF_3)]_3$, or $[Hg(\mu\text{-}C_6F_4)]_3$ fluorinated trimers should make them excellent hole blockers, better so than common organic hole blockers such as BCP (2,9-dimethyl-4,7-diphenylphenanthroline; HOMO = 6.5 eV) or TPBI (1,3,5-tris(*N*-phenylbenzimidazol-2-yl)benzene; HOMO = 6.1 eV). The aforementioned fluorinated trimers should outperform even commercially unavailable perfluorinated organic aromatic compounds such as the $C_{60}F_{42}$ starburst dendrimeric phenylene molecules "CF−Y" and "CF−X" (HOMO = 6.56 and 6.65 eV, respectively), the use of which has enabled OLEDs exhibiting power efficiencies of over 70 lm/W and nearly 100% internal quantum efficiencies.[29]

On the other hand, the proposed device structures in Figure 9 should also achieve exciton blocking from the anode side, due to the shallow LUMO (<1 eV) of the strongly π-basic trimers such as $[Au(\mu\text{-Im-}2CH_3)]_3$. *Furthermore, the HOMO and LUMO energy levels of the metal−organic trimer materials should allow them to serve a dual function such that, in addition to their exciton-blocking role, the π-basic trimers can act as hole transporters while the π-acidic trimers can act as electron transporters.* This should allow the construction of simpler device structures with a smaller number of layers without sacrificing undue barriers for the transport of electrons and holes. For example, the cathode side in the conventional approach for efficient phosphorescent OLEDs contains both an electron transporter, such as Alq_3 (tris-(8-hydroxyquinoline)aluminum; LUMO = 3.2 eV; HOMO = 5.9 eV), and a hole blocker, such as BCP (LUMO = 3.0 eV; HOMO = 6.5 eV). The deeper LUMO of Alq_3 reduces the barrier for electron transport from the cathode, while the deeper HOMO of BCP increases the barrier for holes to propagate past the emissive layer (thus making it a good hole blocker). Thus, layers of both materials are usually required in the conventional device design of phosphorescent OLEDs.[30] In contrast, the device architecture suggested in Figure 9 entails a single layer of a π-acidic trimer $[Ag(\mu\text{-Pz-}2CF_3)]_3$ that can serve both functions even better than the two layers in the conventional approach because this trimer has a LUMO (3.56 eV) that is deeper than that of Alq_3 for the electron-transport function and a HOMO (8.50 eV) that is much deeper than that of BCP for the hole-blocking function! We caution, however, that mobility of electrons and holes, which the computations herein do not predict, are also important in addition to HOMO and LUMO energies.[31]

Summary and Conclusions

Three main effects upon the chemical properties of cyclo-$M_3(\mu\text{-}L)_3$ are studied in this paper: changing the bridging ligand (L), changing the metal (M), and changing the ligand's substituents. For a given coinage metal, changing the bridging ligand yields the following relative π-basicity: $[M(\mu\text{-Im})]_3 > [M(\mu\text{-Py})]_3 > [M(\mu\text{-Cb})]_3 > [M(\mu\text{-Pz})]_3 > [M(\mu\text{-Tz})]_3$. The present study, in addition to previous studies,[9] predicts that the order of basicity is Au > Cu > Ag when changing the metal. As for the substituents on the bridging ligand, the π-basicity can be substantially impacted by inductive effects. Therefore, $[Au(\mu\text{-Im-}2CH_3)]_3$, with an electron-donating group, will produce a strong π-basic trimer, and a strong π-acidic trimer must be $[Ag(\mu\text{-Tz-}2CF_3)]_3$, with a strong electron-withdrawing group. Both the molecular electrostatic potential (MEP) and the positive charge attraction (PCA) calculations show that varying the bridging ligand (L) in the trimer complex most substantially affects the π-basicity character of the complex. The MEP calculations indicate that the π-acidity/basicity results from a ligand-mediated synergism. Upon comparing cyclo-$[M(\mu\text{-L})]_3$ with organic analogues, it is calculated that the former have a much wider range of π-acidity and π-basicity than the former at typical bonding distances.

We close by noting that this research has demonstrated that the π-acidity/basicity of cyclo-$[M(\mu\text{-L})]_3$ can be both coarsely and finely tuned via judicious manipulation of the chemical environment. As a result, one may envision, and calculations presented here support, a wide range of promising optoelectronic applications, such n- and p-type semiconductors for metal−organic field-effect transistors (MOFETs) and exciton blockers for organic light-emitting diodes (OLED) devices. Indeed, the present calculations are guiding ongoing experimental efforts in this direction.

Acknowledgment. The authors acknowledge the U.S. Department of Education for their support of CASCaM. Calculations employed the UNT computational chemistry resource, the purchase of which was supported by a CRIF grant from the U.S. National Science Foundation (CHE-0342824). T.R.C. acknowledges NSF (CHE-0701247) for supporting his contribution. M.A.O. acknowledges partial support of his contribution by the Robert A. Welch Foundation (Grant B-1542), NSF (CHE-0349313), and DOE (DE-FC26-06NT42859). We thank Profs. Bruce Gnade and Nigel Shepherd for helpful discussions.

JA076527U

(28) Gnade, B. E.; Quevedo, M.; Bhansali, U. Unpublished results.
(29) Ikai, M.; Tokito, S.; Sakamoto, Y.; Suzuki, T.; Taga, Y. *Appl. Phys. Lett.* **2001**, *79*, 156.
(30) For reviews, see: (a) Sibley, S.; Thompson, M. E.; Burrows, P. E.; Forrest, S. R. Electroluminescence in Molecular Materials. In *Optoelectronic Properties of Inorganic Compounds;* Roundhill, D. M., Fackler, J. P., Jr., Eds.; Plenum: New York, 1999; Chapter 5. (b) Yersin, H. *Top. Curr. Chem.* **2004**, *241*, 1.
(31) Hung, W.-Y.; Ke, T.-H.; Lin, Y.-T.; Wu, C.-C.; Hung, T.-H.; Chao, T.-C.; Wong, K.-T.; Wu, C.-I. *Appl. Phys. Lett.* **2006**, *88*, 64102.